

## Enhanced adsorption of Ca-ATPase containing vesicles on a negatively charged solid supported membrane for the investigation of membrane transporters

Alessio Sacconi, Maria Rosa Moncelli, Giancarlo Margheri, and Francesco Tadini-Buoninsegni

*Langmuir*, **Just Accepted Manuscript** • Publication Date (Web): 16 Oct 2013

Downloaded from <http://pubs.acs.org> on October 22, 2013

### Just Accepted

“Just Accepted” manuscripts have been peer-reviewed and accepted for publication. They are posted online prior to technical editing, formatting for publication and author proofing. The American Chemical Society provides “Just Accepted” as a free service to the research community to expedite the dissemination of scientific material as soon as possible after acceptance. “Just Accepted” manuscripts appear in full in PDF format accompanied by an HTML abstract. “Just Accepted” manuscripts have been fully peer reviewed, but should not be considered the official version of record. They are accessible to all readers and citable by the Digital Object Identifier (DOI®). “Just Accepted” is an optional service offered to authors. Therefore, the “Just Accepted” Web site may not include all articles that will be published in the journal. After a manuscript is technically edited and formatted, it will be removed from the “Just Accepted” Web site and published as an ASAP article. Note that technical editing may introduce minor changes to the manuscript text and/or graphics which could affect content, and all legal disclaimers and ethical guidelines that apply to the journal pertain. ACS cannot be held responsible for errors or consequences arising from the use of information contained in these “Just Accepted” manuscripts.



1  
2  
3  
4  
5 Enhanced adsorption of Ca-ATPase containing  
6  
7  
8  
9 vesicles on a negatively charged solid supported  
10  
11  
12  
13 membrane for the investigation of membrane  
14  
15  
16  
17 transporters  
18  
19  
20  
21  
22  
23  
24

25 *Alessio Sacconi<sup>1</sup>, Maria Rosa Moncelli<sup>1</sup>, Giancarlo Margheri<sup>2</sup>, Francesco Tadini-Buoninsegni<sup>1\*</sup>*  
26  
27  
28  
29  
30  
31

32 <sup>1</sup>Department of Chemistry “Ugo Schiff”, University of Florence, via della Lastruccia 3, 50019 Sesto  
33  
34 Fiorentino, Italy.

35  
36 <sup>2</sup>Institute for Complex Systems, National Research Council, Via Madonna del Piano 10, 50019  
37  
38 Sesto Fiorentino, Italy.  
39  
40  
41  
42  
43  
44  
45  
46  
47  
48  
49  
50  
51  
52  
53  
54  
55  
56  
57  
58  
59  
60

1  
2  
3  
4  
5  
6  
7  
8  
9  
10  
11  
12  
13  
14  
15  
16  
17  
18  
19  
20  
21  
22  
23  
24  
25  
26  
27  
28  
29  
30  
31  
32  
33  
34  
35  
36  
37  
38  
39  
40  
41  
42  
43  
44  
45  
46  
47  
48  
49  
50  
51  
52  
53  
54  
55  
56  
57  
58  
59  
60  
ABSTRACT

A convenient model system for a biological membrane is a solid supported membrane (SSM), which consists of a gold-supported alkanethiol|phospholipid bilayer. In combination with a concentration jump method, SSMs have been used for the investigation of several membrane transporters. Vesicles incorporating sarcoplasmic reticulum Ca-ATPase (SERCA) were adsorbed on a negatively charged SSM (octadecanethiol|phosphatidylserine bilayer). The current signal generated by the adsorbed vesicles following an ATP concentration jump was compared to that produced by SERCA containing vesicles adsorbed on a conventional SSM (octadecanethiol|phosphatidylcholine bilayer). A significantly higher current amplitude was recorded on the serine-based SSM. The adsorption of SERCA incorporating vesicles on the SSM was then characterized by surface plasmon resonance (SPR). The SPR measurements clearly indicate that in the presence of  $\text{Ca}^{2+}$  and  $\text{Mg}^{2+}$  the amount of adsorbed vesicles on the serine-based SSM is about twice that obtained using the conventional SSM, thereby demonstrating that the higher current amplitude recorded on the negatively charged SSM is correlated with a greater quantity of adsorbed vesicles. The enhanced adsorption of membrane vesicles on the PS-based SSM may be useful to study membrane preparations with a low concentration of transport protein generating small current signals, as in the case of various recombinantly expressed proteins.

## INTRODUCTION

A convenient model system for a biological membrane is a solid supported membrane (SSM), which has been employed for the functional characterization of several membrane transport proteins (1,2). The SSM consists of a hybrid alkanethiol|phospholipid bilayer supported by a gold electrode. In particular, the SSM is formed by an octadecanethiol (Oct) monolayer covalently bound to the gold surface via the sulphhydryl group and a second phosphatidylcholine monolayer on top of the

1 thiol layer. In combination with a concentration jump method (3), SSMs have successfully been  
2 used to study electrogenic transport by ion pumps (3-6), secondary active transporters (7,8) and ion  
3 channels (9-12).  
4  
5  
6  
7

8 In the concentration jump method, membrane preparations (membrane fragments or vesicles)  
9 containing the protein of interest are adsorbed on a SSM, which is usually formed by a diphytanoyl  
10 phosphatidylcholine (PC) monolayer on top of the gold-supported Oct film (1-3). However, it has  
11 not been demonstrated whether this is definitely the SSM sensor that adsorbs the higher amount of  
12 membrane vesicles. Aiming to fabricate a SSM with higher affinity to vesicles with incorporated  
13 membrane transporters, a possible strategy would be that of using a lipid surface of different  
14 composition and charge, i.e. different lipid head groups. It is known that negatively charged lipid  
15 headgroups can strongly interact with bivalent cations (13-17), e.g.  $\text{Ca}^{2+}$  and  $\text{Mg}^{2+}$ , which were  
16 reported to promote the adsorption process of small unilamellar phospholipid vesicles on a gold-  
17 supported organophosphate monolayer (18). However, the adsorption of protein containing  
18 membrane vesicles on a negatively charged SSM has not yet been investigated. For this purpose, in  
19 this work we characterized a new SSM based on diphytanoyl phosphatidylserine (PS), which has  
20 the same hydrophobic moiety as that of PC, that is the model molecule to be compared, but a final  
21 negatively charged serine headgroup (19). By employing the concentration jump method, we  
22 compared the current signal produced by vesicles containing sarcoplasmic reticulum Ca-ATPase  
23 (SERCA) adsorbed on our new SSM (Oct|PS bilayer) with that obtained with SERCA incorporating  
24 vesicles adsorbed on the conventional SSM (Oct|PC bilayer). A SERCA-generated current transient  
25 with much higher amplitude was recorded on the PS-based SSM. To explain this result, the  
26 adsorption of SERCA containing vesicles on the SSM was investigated by surface plasmon  
27 resonance (SPR) measurements in the presence and absence of  $\text{Ca}^{2+}$  and  $\text{Mg}^{2+}$  ions. We found that  
28  $\text{Ca}^{2+}$  and  $\text{Mg}^{2+}$  have a fundamental role in the adsorption of SERCA containing vesicles on the SSM  
29  
30  
31  
32  
33  
34  
35  
36  
37  
38  
39  
40  
41  
42  
43  
44  
45  
46  
47  
48  
49  
50  
51  
52  
53  
54  
55  
56  
57  
58  
59  
60

1 surface. We demonstrate that the higher current peak measured on the PS-based SSM is strictly  
2 correlated with a greater amount of adsorbed vesicles.  
3  
4  
5  
6  
7  
8  
9

## 10 MATERIALS and METHODS

11 The lipid solution contained 1,2-glycero diphytanoyl-sn-3-[phospho-L-choline] (PC) or 1,2-  
12 glycero diphytanoyl-sn-3-[phospho-L-serine] (PS) (Avanti Polar Lipids) and was prepared at a  
13 concentration of 7.5 mg/mL in n-decane or n-octane (Merck).  
14  
15  
16  
17  
18

19 Native sarcoplasmic reticulum (SR) vesicles containing SERCA were prepared as reported by  
20 Eletr and Inesi (20). The total protein concentration, determined by the Lowry procedure (21), was  
21 8.4 mg/ml. SERCA content corresponds to ~50% of the total protein (22).  
22  
23  
24  
25

26 COS-1 microsomes incorporating recombinant wild type (WT) SERCA were obtained as  
27 previously described (23). Total protein concentration was 2.6 mg/ml (78  $\mu$ g/ml of SERCA  
28 corresponding to 3%). The content of expressed SERCA was evaluated by SDS gel electrophoresis  
29 and Western blots (23).  
30  
31  
32  
33  
34  
35  
36

### 37 Concentration jump method

38 The SSM was formed as described (3) using a PC or PS solution (7.5mg/mL) in n-decane. In each  
39 experiment we added to the SSM the same amount of native SR vesicles or SERCA-incorporating  
40 COS-1 microsomes. The vesicles were then adsorbed on the SSM during an incubation time of 90  
41 minutes. Following adsorption, SERCA was activated by an ATP concentration jump. If at least one  
42 electrogenic step, i.e. a net charge movement across the vesicular membrane generated by the  
43 protein, is involved in the relaxation process following protein activation, a current transient can be  
44 recorded due to the capacitive coupling between vesicle membrane and SSM (1,24). In particular,  
45 the current signal of the membrane transporter can be detected under potentiostatic conditions. In  
46  
47  
48  
49  
50  
51  
52  
53  
54  
55  
56  
57  
58  
59  
60

1 this case, movement of a net charge across the activated protein is compensated by a flow of  
2  
3  
4 electrons along the external circuit toward the gold electrode surface to keep the applied voltage  $\Delta V$   
5  
6 constant across the whole metal/solution interphase. The resulting current transient is recorded as a  
7  
8 function of time. Normally, experiments are carried out under short circuit-conditions, i.e. at zero  
9  
10 applied voltage relative to the reference electrode. The numerically integrated current transient is  
11  
12 related to a net charge movement within the protein, which depends upon the particular electrogenic  
13  
14 step.  
15

16  
17 In ATP concentration jumps the buffer solution contained 100 mM choline chloride, 25 mM  
18  
19 MOPS, (pH 7.0), 1 mM MgCl<sub>2</sub>, 0.25 mM EGTA, 0.25 mM CaCl<sub>2</sub> (10 μM free Ca<sup>2+</sup>) and 0.2 mM  
20  
21 DTT. Activation was obtained by rapid addition of 100 μM ATP.  
22

23  
24 The concentration jump experiments were performed by the SURFE<sup>2</sup>R<sup>One</sup> device (Nanon  
25  
26 Technologies). The temperature was maintained at 22-23 °C for all the experiments.  
27

28  
29 To verify the reproducibility of the current transients on the same SSM, each single measurement  
30  
31 was repeated 6 times (two minute waiting time after each measurement) and then averaged to  
32  
33 improve the signal to noise ratio. Standard deviations did not exceed 5%. Moreover, each set of  
34  
35 measurements was usually reproduced using three different SSM sensors.  
36  
37

38  
39 SPR and electrochemical measurements combined in situ  
40

41  
42 All electrochemical and SPR measurements were performed using the templated stripped gold  
43  
44 (TSG) sensors purchased from Restec (Resonant Sensor Technology). The TSG sensor was  
45  
46 incubated in a solution of 0.2 mM Oct in ethanol for 16 hours to allow Oct monolayer formation on  
47  
48 the TSG surface by self assembly. The TSG sensor was then rinsed with ethanol to remove thiol  
49  
50 molecules not covalently bound to the gold surface. The sensor was finally dried under a stream of  
51  
52 N<sub>2</sub> and was oil-matched to the base of a 45° roof LaSFN9 glass prism (Hellma Optik; dielectric  
53  
54 constant  $n = 1.85$  at  $\lambda = 633$  nm). By means of an O-ring tight seal, the thiol-coated TSG sensor was  
55  
56  
57  
58  
59  
60

1  
2  
3  
4  
5  
6  
7  
8  
9  
10  
11  
12  
13  
14  
15  
16  
17  
18  
19  
20  
21  
22  
23  
24  
25  
26  
27  
28  
29  
30  
31  
32  
33  
34  
35  
36  
37  
38  
39  
40  
41  
42  
43  
44  
45  
46  
47  
48  
49  
50  
51  
52  
53  
54  
55  
56  
57  
58  
59  
60

mounted in a Teflon cell for in situ electrochemical and SPR analysis using the Kretschmann configuration. After cell assembling, a phospholipid layer was formed by spreading 40  $\mu\text{L}$  of a phospholipid (PC or PS) solution (7.5 mg/mL) in n-octane on top of the gold-supported Oct monolayer. Following phospholipid addition, the cell was immediately filled with a buffer solution, whose composition, ionic strength and pH were the same as in the case of current transient measurements. Formation of the gold-supported alkanethiol|phospholipid bilayer (Au|Oct|PC or Au|Oct|PS) usually occurred during an incubation time of 16 hours. After SSM formation, the cell was placed on a rotating stage in a  $\theta$ -2 $\theta$  configuration. The monochromatic light beam from a He/Ne laser (JDS Uniphase;  $\lambda = 632.8$  nm, beam diameter = 480  $\mu\text{m}$ ) was focused into the cell through the prism, and the reflected light was collected by a photodiode detector (25). The software Wasplas (A. Scheller, Max Planck Institute for Polymer Research, Mainz, Germany) was used for SPR measurements.

We characterized the SSM by AC Voltammetry and Electrochemical Impedance Spectroscopy (EIS). The electrochemical measurements were performed using a PGSTAT12 Autolab potentiostat/galvanostat (Metrohm), with an in-built frequency response analysis FRA2module. All potentials were referred to a three electrode system, with an Ag|AgCl|0.1 M KCl homemade reference electrode, a Pt electrode as a counter-electrode and the TSG as the working electrode. Capacitance and resistance of the SSM were determined by AC Voltammetry (potential range from 0.0 to + 0.10 V combined with a superimposed wave of 75 Hz frequency and 10 mV amplitude, and in a phase setting of 90° to obtain the capacitive signal) and EIS (bias potential 0.0 V, frequency range from 10<sup>5</sup> to 10<sup>-2</sup> Hz with 10 mV amplitude). Following formation and characterization of the SSM, the buffer solution in the cell was exchanged with a suspension of native SR vesicles or COS-1 microsomes. In each adsorption experiment the amount of SR vesicles or COS-1 microsomes added to the cell was the same as indicated for the corresponding concentration jump experiment. After an incubation time of 90 minutes, the cell was rinsed three times, every 40 minutes, with 5 mL

1 of buffer solution to remove scarcely bound vesicles. This volume guarantees the complete  
2 exchange of buffer solution in the cell. The fixed angle of incidence ( $56.00^\circ$ ) was chosen at the  
3 lower flank of the decreasing reflectivity before the SPR peak. The percentage of the reflectivity  
4 ( $\%R$ ) registered at the fixed angle of incidence was reported as a function of time. The plasma angle  
5 shift ( $\Delta\theta$ ) was given by the difference between the plasma angle value after the third rinse and the  
6 plasma angle value before vesicles injection.  
7  
8  
9  
10  
11  
12  
13  
14  
15  
16  
17  
18

## 19 RESULTS and DISCUSSION

### 20 Current transient measurements

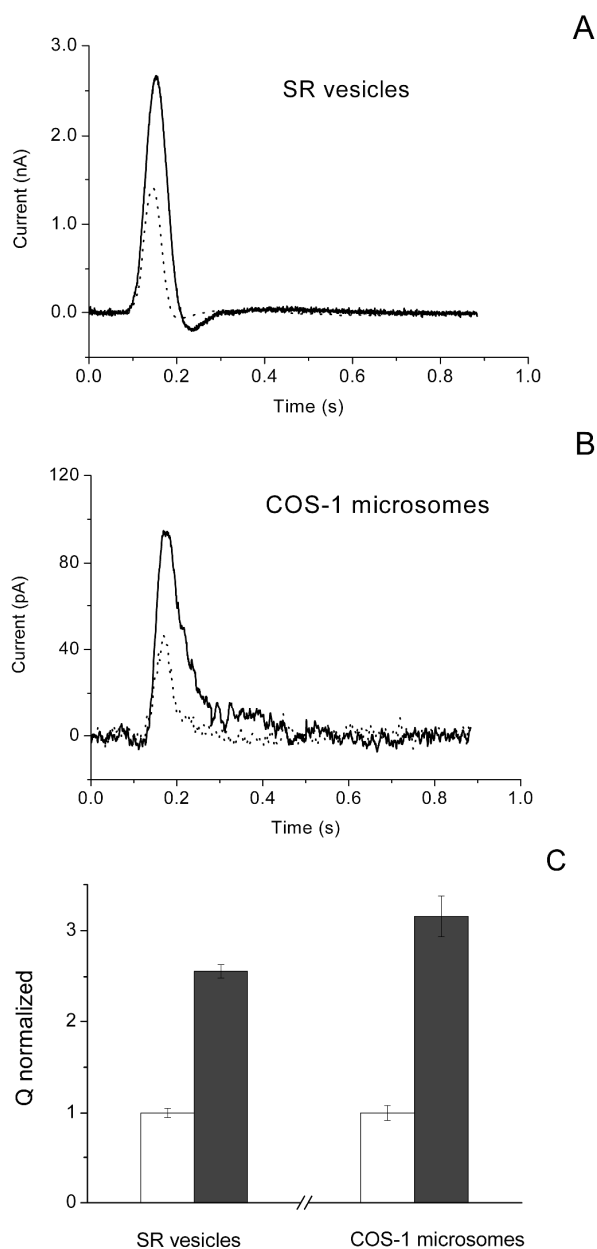
21  
22 The SERCA protein has been extensively investigated by the concentration jump method based  
23 on current transient measurements (1,4,23,24). This enzyme, which is a prominent and well  
24 characterized member of the P-type ATPase family, couples the hydrolysis of one molecule of ATP  
25 to the active transport of two  $\text{Ca}^{2+}$  ions from the cytoplasm to the SR lumen in muscle cells (22,26).  
26  
27  
28  
29  
30  
31

32 In this study, SR vesicles containing native SERCA (Fig. 1A) were adsorbed on a SSM, i.e. gold-  
33 supported Oct|PC or Oct|PS bilayer, and subjected to ATP activation. If we performed a 100  $\mu\text{M}$   
34 ATP jump in the presence of 10  $\mu\text{M}$  free  $\text{Ca}^{2+}$  and 1 mM  $\text{Mg}^{2+}$ , we observed a current transient,  
35 whose related charge has been attributed to an electrogenic event corresponding to movement of  
36 bound  $\text{Ca}^{2+}$  within the enzyme following utilization of ATP (24). In control experiments on native  
37 SR vesicles adsorbed on the PS- and PC-based SSM we confirmed that the ATP-induced current  
38 transient measured in the presence of  $\text{Ca}^{2+}$  was fully suppressed by 100 nM thapsigargin (TG), a  
39 highly specific and potent SERCA inhibitor (27,28), as previously reported (24). It is interesting to  
40 note that in the case of native SR vesicles adsorbed on a Oct|PS bilayer (Fig. 1A, solid line) the  
41 amplitude of the current peak is significantly higher with respect to that measured on a Oct|PC  
42 bilayer (Fig. 1A, dotted line). By numerically integrating the current transient recorded on the  
43  
44  
45  
46  
47  
48  
49  
50  
51  
52  
53  
54  
55  
56  
57  
58  
59  
60



1  
2  
3  
4  
5  
6  
7  
8  
9  
10  
11  
12  
13  
14  
15  
16  
17  
18  
19  
20  
21  
22  
23  
24  
25  
26  
27  
28  
29  
30  
31  
32  
33  
34  
35  
36  
37  
38  
39  
40  
41  
42  
43  
44  
45  
46  
47  
48  
49  
50  
51  
52  
53  
54  
55  
56  
57  
58  
59  
60

Oct|PS bilayer, we found a value for the related charge, which is approximately 2.7 times higher than that obtained on the Oct|PC bilayer (Fig. 1C). It should be pointed out that the current peak value is related to the number of adsorbed ATPase molecules that are activated after the ATP concentration jump, and the charge obtained by numerical integration corresponds to the overall amount of  $\text{Ca}^{2+}$  ions traslocated by the ion pumps following their activation.



1 **Figure 1.** Currents transients induced by 100 $\mu$ M ATP concentration jumps in the presence of 10  $\mu$ M  
2 free  $\text{Ca}^{2+}$  and 1 mM  $\text{Mg}^{2+}$  using native SR vesicles containing SERCA (A) or COS-1 microsomes  
3 incorporating recombinant WT SERCA (B) adsorbed on a gold-supported Oct|PC (dotted line) or  
4 Oct|PS (solid line) bilayer. (C) Normalized charges related to current transients by native SR  
5 vesicles containing SERCA or COS-1 microsomes incorporating recombinant WT SERCA  
6 adsorbed on a Oct|PC (white columns) or Oct|PS (dark grey columns) bilayer. The charges were  
7 normalized to the charge obtained on the Oct|PC bilayer. The error bars represent the s.e.m. of three  
8 independent measurements.  
9  
10  
11  
12  
13  
14  
15  
16  
17  
18  
19

20  
21 The concentration jump method has been employed to investigate not only native SERCA, but  
22 also the recombinant WT and mutant enzyme expressed in microsomes of COS-1 cells (23). The  
23 study of recombinant mutant SERCA provided useful information for a detailed characterization of  
24 the enzyme's transport cycle, especially as concerns  $\text{Ca}^{2+}$  binding mechanism,  $\text{Ca}^{2+}/\text{H}^{+}$  exchange  
25 and competitive  $\text{Mg}^{2+}$  binding (23). To examine the effects of a negatively charged SSM surface on  
26 the current signal generated by recombinant WT SERCA, COS-1 microsomes were adsorbed on a  
27 Oct|PS bilayer and activated by an ATP concentration jump. Similarly to native SERCA, we found  
28 that the current peak generated by recombinant WT SERCA on a Oct|PS bilayer (Fig. 1B, solid line)  
29 is characterized by a much higher amplitude with respect to that measured on the conventional  
30 SSM, i.e. Oct|PC bilayer (Fig. 1B, dotted line). Also in the case of recombinant SERCA the ATP-  
31 induced current transient recorded on the Oct|PS or Oct|PC bilayer was totally abolished by 100nM  
32 TG, thereby confirming again that the measured current transient is related to transport of  $\text{Ca}^{2+}$  ions  
33 by the SERCA enzyme. Moreover, the charge related to the current transient on the PS-based SSM  
34 was found to be about three times higher than that observed on the PC-based SSM (Fig. 1C).  
35  
36  
37  
38  
39  
40  
41  
42  
43  
44  
45  
46  
47  
48  
49  
50  
51  
52  
53  
54  
55  
56  
57  
58  
59  
60

1 concentration in COS-1 microsomes (78  $\mu\text{g}/\text{ml}$ ) is much lower than that in SR vesicles ( $\sim 4.2$   
2  
3  
4  $\text{mg}/\text{ml}$ ).

5  
6 In conclusion, for both SR vesicles and COS-1 microsomes a much higher current peak was  
7  
8 measured when the protein was adsorbed on an Oct|PS bilayer. This increase in the current signal  
9  
10 may be explained by a greater quantity of adsorbed vesicles on the PS-based SSM.  
11

#### 12 13 14 15 In-situ SPR and electrochemical measurements

16  
17 In order to verify the above statement, vesicles adsorption on the SSM was studied using SPR and  
18  
19 electrochemical techniques (EIS and AC voltammetry) combined in situ. We investigated the  
20  
21 adsorption of native SR vesicles or COS-1 microsomes on Au|Oct|PC or Au|Oct|PS sensors in the  
22  
23 presence or absence of  $\text{Ca}^{2+}$  and  $\text{Mg}^{2+}$ . The concentration of  $\text{Ca}^{2+}$  and  $\text{Mg}^{2+}$ , as well as the ionic  
24  
25 strength and pH of the buffer solution, were the same as in the case of the current transient  
26  
27 measurements.  
28  
29

30  
31 Before vesicles adsorption on the SSM, the Au|Oct, Au|Oct|PC and Au|Oct|PS systems were  
32  
33 characterized by AC and EIS techniques to evaluate in situ the correct formation and stability of the  
34  
35 alkanethiol monolayer and the alkanethiol|phospholipid bilayer. Both the monolayer and the bilayer  
36  
37 can be described by an equivalent circuit which consists of a parallel RC mesh in series with a  
38  
39 solution resistance (Fig. S1 in Supporting Information) (29,30). In particular, the capacitance and  
40  
41 resistance values (Table 1) of the monolayer and bilayer can be obtained by fitting the equivalent  
42  
43 circuit to the EIS data (Fig. S1 in Supporting Information).  
44  
45  
46  
47  
48  
49  
50  
51  
52  
53  
54  
55  
56  
57  
58  
59  
60

|                  | $R_{\text{solution}}^{(a)}$<br>( $\Omega \cdot \text{cm}^2$ ) | $R^{(a)}$<br>( $M\Omega \cdot \text{cm}^2$ ) | $C^{(a)}$<br>( $\mu\text{F}/\text{cm}^2$ ) | $C^{(b)}$<br>( $\mu\text{F}/\text{cm}^2$ ) |
|------------------|---------------------------------------------------------------|----------------------------------------------|--------------------------------------------|--------------------------------------------|
| <b>Au Oct</b>    | $50.0 \pm 1.0$                                                | $1.50 \pm 0.30$                              | $1.05 \pm 0.10$                            | $1.20 \pm 0.10$                            |
| <b>Au Oct PC</b> | $50.0 \pm 1.0$                                                | $7.00 \pm 1.5$                               | $0.34 \pm 0.05$                            | $0.37 \pm 0.05$                            |
| <b>Au Oct PS</b> | $50.0 \pm 2.0$                                                | $23.5 \pm 8.0$                               | $0.32 \pm 0.04$                            | $0.32 \pm 0.20$                            |

**Table 1.** Resistance and capacitance values of gold-supported Oct monolayer and Oct|PC or Oct|PS bilayer were obtained by EIS spectroscopy (a) and AC voltammetry (b). The solution resistance was determined by EIS. The EIS error gives the deviation from the fit and the error in the AC voltammetry data represents the s.e.m. of four independent measurements.

The capacitance of the monolayer and bilayer was also evaluated by AC voltammetry (Fig. S2 in Supporting Information), yielding values very similar to those determined by EIS (Table 1). From our AC voltammetry data, that were obtained in a phase setting of  $90^\circ$ , the resistance value cannot be determined. The slightly higher resistance of Au|Oct|PS with respect to that of Au|Oct|PC is probably due to the higher compactness of the PS-based bilayer, which is presumably related to the presence of  $\text{Ca}^{2+}$  and  $\text{Mg}^{2+}$  ions interposed between the negatively charged serine headgroups. The capacitance and resistance values in Table 1 are in good agreement with those reported in the literature (31-36), thus confirming the proper formation and integrity of the thiol monolayer and the hybrid thiol|phospholipid bilayer.

1  
2 After monitoring the correct formation of the SSM on the sensor surface, we performed SPR  
3  
4 measurements to characterize the adsorption of SERCA containing vesicles on the  
5  
6 alkanethiol|phospholipid bilayer. Figures 2A and 2B show the SPR kinetic curves of the reflectivity  
7  
8 signal versus time for native SR vesicles adsorption on Au|Oct|PC or Au|Oct|PS, respectively. For  
9  
10 both sensors, we compared the adsorption process in the presence of 10  $\mu\text{M}$   $\text{Ca}^{2+}$  and 1 mM  $\text{Mg}^{2+}$   
11  
12 (solid lines), and in absence of both ions (dotted lines). When the SSM was completely formed and  
13  
14 stabilized, the incidence angle was set at  $56.00^\circ$  obtaining the corresponding reflectivity value of  
15  
16  $\sim 30\%$ , that represents the baseline of the reflectivity signal before SR vesicles addition.  
17  
18

19  
20 After SR vesicles injection in the cell, the reflectivity signal progressively increased during the  
21  
22 incubation time and finally attained a maximum constant value. Such an increase in reflectivity  
23  
24 clearly indicates the occurrence of SR vesicles adsorption on the SSM surface. It is interesting to  
25  
26 observe that in the presence of  $\text{Ca}^{2+}$  and  $\text{Mg}^{2+}$  ions a greater quantity of SR vesicles was adsorbed  
27  
28 on the PS-based SSM (Fig. 2B, solid line) with respect to the PC-based SSM (Fig. 2A, solid line).  
29  
30 In the absence of  $\text{Ca}^{2+}$  and  $\text{Mg}^{2+}$  ions, very few SR vesicles, if any, were adsorbed on the PC or PS-  
31  
32 based SSM (Figs. 2A and 2B, dotted lines).  
33  
34  
35  
36  
37  
38  
39  
40  
41  
42  
43  
44  
45  
46  
47  
48  
49  
50  
51  
52  
53  
54  
55  
56  
57  
58  
59  
60

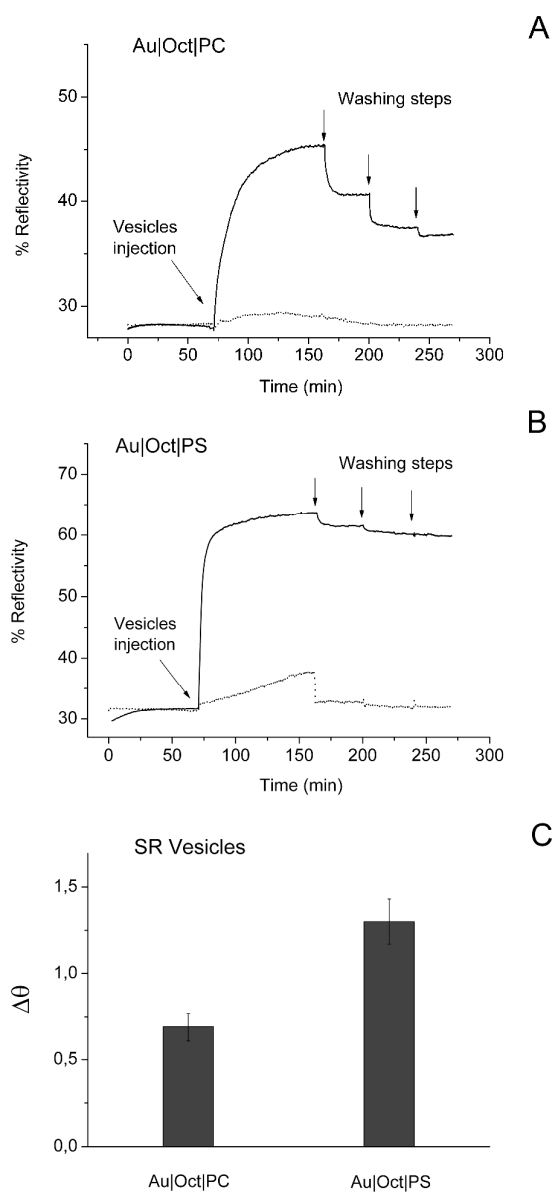


**Figure 2.** Reflectivity versus time kinetic curves for the adsorption process of native SR vesicles on Au|Oct|PC (A) or Au|Oct|PS (B) sensor in the presence (solid line) and in the absence (dotted line) of  $\text{Ca}^{2+}$  and  $\text{Mg}^{2+}$ . (C) The histogram shows the plasma angle shift ( $\Delta\theta$ ) values for SR vesicles adsorption on Au|Oct|PC or Au|Oct|PS sensor in the presence of  $\text{Ca}^{2+}$  and  $\text{Mg}^{2+}$ . The vertical bars represent the reproducibility errors of three independent measurements.

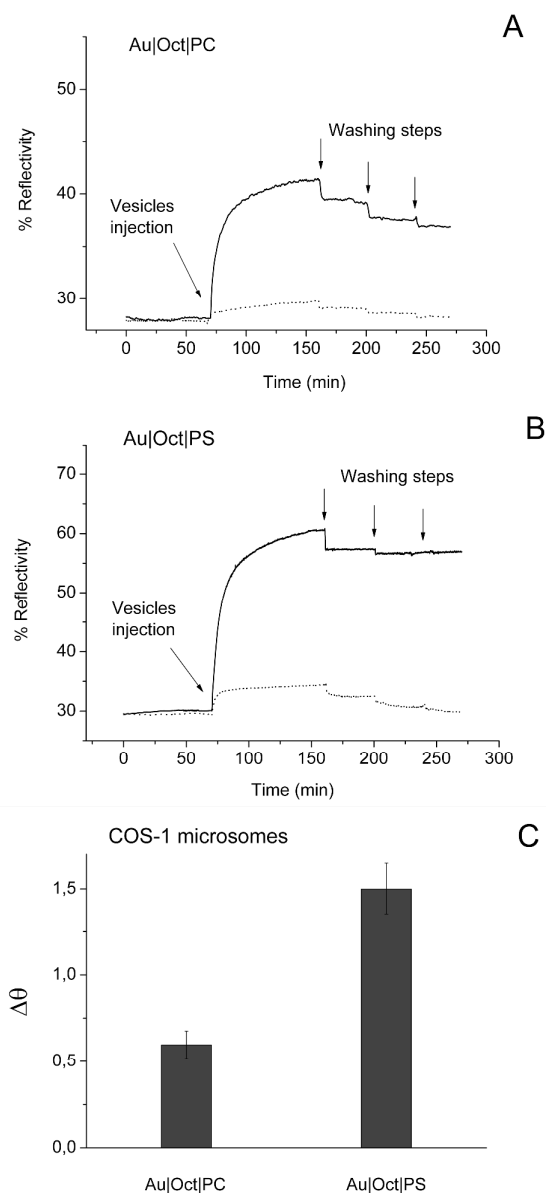
1  
2 Interestingly, we found that the adsorption process in the presence of PC (Fig. 2A, solid line)  
3 occurs in longer times than those occurring in the presence of PS (Fig. 2B, solid line). For example,  
4 in the presence of both  $\text{Ca}^{2+}$  and  $\text{Mg}^{2+}$  the risetime of the reflectivity signal is  $\sim 890$  s using PC on  
5 the sensor surface, while it reduces to  $\sim 260$  s in the case of PS, confirming the tendency of SR  
6 vesicles to bind preferentially to the PS-based SSM rather than the PC-based SSM and, therefore,  
7 indicating a higher affinity of the SR vesicles for the negatively charged SSM, as expected.  
8  
9

10  
11 As the cell was further rinsed with the buffer solution, we recorded a decrease of the reflectivity  
12 signal which can be explained by partial removal of the SR vesicles from the SSM surface. In the  
13 presence of  $\text{Ca}^{2+}$  and  $\text{Mg}^{2+}$  ions (solid lines), such a decrease in reflectivity is less evident when the  
14 SSM is formed with PS (Fig. 2B) rather than PC (Fig. 2A). Moreover, the reflectivity decrease after  
15 the rinsing steps is systematically lower for PS than for PC. This is a further indication of the higher  
16 affinity of the SR vesicles for the PS-based SSM.  
17  
18

19  
20 We can compare the amount of adsorbed SR vesicles on the PC and PS-based SSM by  
21 determining the values of the plasma angle shift  $\Delta\theta$ , as this quantity is directly proportional to the  
22 adsorbed mass (37). The histogram (Fig 2C) shows that the amount of native SR vesicles adsorbed  
23 on the Au|Oct|PS sensor surface is approximately twice that obtained on the Au|Oct|PC sensor, in  
24 the presence of  $\text{Ca}^{2+}$  and  $\text{Mg}^{2+}$  ions. This result is consistent with the current signal increase  
25 observed with SR vesicles adsorbed on the PS-based SSM (Fig. 1A). It is worth noticing that in the  
26 absence of both ions the  $\Delta\theta$  values are close to zero.  
27  
28

29  
30 The experimental procedure described above was then repeated using COS-1 microsomes.  
31 Figures 3A and 3B show the reflectivity versus time kinetic curves for COS-1 microsomes  
32 adsorption on Au|Oct|PC or Au|Oct|PS, respectively. Also in the case of COS-1 microsomes, we  
33 observed that in the presence of  $\text{Ca}^{2+}$  and  $\text{Mg}^{2+}$  a greater quantity of vesicles can be adsorbed on the  
34 PS-based SSM (Fig. 3B) with respect to the PC-based SSM (Fig. 3A). In the absence of bivalent  
35 cations, a very low amount of vesicles is adsorbed on the SSM and the adsorbed vesicles can be  
36  
37  
38  
39  
40  
41  
42  
43  
44  
45  
46  
47  
48  
49  
50  
51  
52  
53  
54  
55  
56  
57  
58  
59  
60

1 completely removed from the SSM surface following buffer rinsing (Figs. 3A and 3B, dotted lines).  
2  
3 We note that the risetimes of the reflectivity signals don't exhibit a marked difference as that  
4  
5 observed for native SR vesicles (Figs. 2A and 2B). Among the various reasons that reduce this  
6  
7 effect, we suggest that the different total protein concentration in the SR vesicles and COS-1  
8  
9 microsomes may play a role, as the association rates are concentration-dependent.  
10  
11  
12  
13  
14  
15  
16  
17  
18  
19  
20  
21  
22  
23  
24  
25  
26  
27  
28  
29  
30  
31  
32  
33  
34  
35  
36  
37  
38  
39  
40  
41  
42  
43  
44  
45  
46  
47  
48  
49  
50  
51  
52



53 **Figure 3.** Reflectivity versus time kinetic curves for the adsorption process of COS-1 microsomes  
54 on Au|Oct|PC (A) or Au|Oct|PS (B) sensor in the presence (solid line) and in the absence (dotted  
55  
56  
57  
58  
59  
60



1  
2 line) of  $\text{Ca}^{2+}$  and  $\text{Mg}^{2+}$ . (C) The histogram shows the plasma angle shift ( $\Delta\theta$ ) values for COS-1  
3  
4 microsomes adsorption on Au|Oct|PC or Au|Oct|PS sensor in the presence of  $\text{Ca}^{2+}$  and  $\text{Mg}^{2+}$ . The  
5  
6 vertical bars represent the reproducibility errors of three independent measurements.  
7  
8

9  
10 In the case of COS-1 microsomes, the  $\Delta\theta$  value due to microsomes adsorption by PS is  
11  
12 approximately 2.5 times higher than that obtained with PC (Fig. 3C), also in this case consistent  
13  
14 with the current signal increase detected on the PS-based SSM (Fig. 1B).  
15  
16

17 From our SPR measurements it is therefore evident the strong influence of  $\text{Ca}^{2+}$  and  $\text{Mg}^{2+}$  in the  
18  
19 adsorption process of membrane vesicles on the SSM surface. The higher current peak recorded on  
20  
21 the PS-based SSM can be correlated with a greater amount of adsorbed vesicles on the Au|Oct|PS  
22  
23 sensor in the presence of  $\text{Ca}^{2+}$  and  $\text{Mg}^{2+}$ . On the other hand, without  $\text{Ca}^{2+}$  and  $\text{Mg}^{2+}$ , the adsorption  
24  
25 of membrane vesicles on the SSM is drastically reduced and all adsorbed vesicles can be easily  
26  
27 removed from the SSM surface.  
28  
29  
30  
31  
32  
33  
34

## 35 CONCLUSIONS

36  
37 The current signal generated by SERCA containing vesicles adsorbed on a negatively charged  
38  
39 SSM (Oct|PS bilayer) following an ATP concentration jump exhibits a much higher amplitude with  
40  
41 respect to that produced by SR vesicles adsorbed on a conventional SSM (Oct|PC bilayer). The SPR  
42  
43 measurements clearly indicate that in the presence of  $\text{Ca}^{2+}$  and  $\text{Mg}^{2+}$  the amount of adsorbed  
44  
45 vesicles on our new PS-based SSM is about twice that obtained using the conventional PC-based  
46  
47 SSM, thereby demonstrating that the higher current amplitude recorded on the negatively charged  
48  
49 SSM is correlated with a greater quantity of adsorbed vesicles.  
50  
51

52 It is known that  $\text{Ca}^{2+}$  and  $\text{Mg}^{2+}$  ions can strongly interact with negatively charged phospholipid  
53  
54 headgroups, as previously reported (13-18). The accumulation of cations at the negatively charged  
55  
56  
57  
58  
59  
60

1 SSM surface may contribute to a more stable vesicles-SSM interaction. We suggest that  $\text{Ca}^{2+}$  and  
2  
3  $\text{Mg}^{2+}$  coordinated to serine headgroups of the PS-based SSM may promote a further interaction with  
4  
5 the external surface of the membrane vesicles. It is worth noticing that the external surface of the  
6  
7 SR vesicle is the cytoplasmic surface of the SR. Since the cytoplasmic leaflet of membranes  
8  
9 contains significant amount of phosphatidylserine, we propose that  $\text{Ca}^{2+}$  and  $\text{Mg}^{2+}$  ions may bind to  
10  
11 both serine-rich membranes and connect them. The coordinating effect of  $\text{Ca}^{2+}$  and  $\text{Mg}^{2+}$  ions may  
12  
13 be regarded as a type of “ionic glue”, as proposed for  $\text{Zr}^{4+}$  cations (38). In this connection, it is  
14  
15 useful to compare the coordination number (CN) of  $\text{Zr}^{4+}$  (CN = 7 and 8) with those of  $\text{Mg}^{2+}$  (CN =  
16  
17 5 and 6) and  $\text{Ca}^{2+}$  (CN = 6 and 7) (39). However, the studies on the interaction of  $\text{Zr}^{4+}$  ions with  
18  
19 various phospholipid headgroups (40-42) indicate that  $\text{Zr}^{4+}$ , due to its high ionic charge and specific  
20  
21 coordination properties, interacts with lipid headgroups more strongly and effectively than divalent  
22  
23 cations, such as  $\text{Mg}^{2+}$  and  $\text{Ca}^{2+}$ . Therefore, the term “ionic super glue” (38) appears most  
24  
25 appropriate for the coordinating behavior of  $\text{Zr}^{4+}$  ions.  
26  
27  
28  
29

30 The enhanced adsorption of membrane vesicles on the PS-based SSM may be particularly useful  
31  
32 to study membrane preparations with a low concentration of transport protein generating very small  
33  
34 amplitudes in current recordings, as demonstrated here for the recombinantly expressed Ca-ATPase.  
35  
36  
37  
38  
39  
40

#### 41 ACKNOWLEDGMENTS

42  
43 The authors wish to thank Dr. Gianluca Bartolommei for very helpful suggestions and critical  
44  
45 reading of the manuscript, and Dr. Giuseppe Inesi for providing them with recombinant SERCA.  
46  
47 Financial support by Ente Cassa di Risparmio di Firenze (2009.0749) and the Italian Ministry of  
48  
49 Education, University and Research (PRIN Project 20083YM37E) is gratefully acknowledged.  
50  
51  
52  
53  
54  
55  
56  
57  
58  
59  
60

1 **Supporting Information Available.** Electrochemical characterization (Electrochemical Impedance  
2 Spectroscopy and AC Voltammetry) of the octadecanethiol monolayer and  
3  
4 octadecanethiol|phosphatidylcholine or octadecanethiol|phosphatidylserine bilayer supported by  
5  
6 gold. This information is available free of charge via the Internet at <http://pubs.acs.org/>.  
7  
8  
9

### 10 11 12 13 14 15 **Corresponding Author**

16  
17 \*Francesco Tadini-Buoninsegni, Department of Chemistry “Ugo Schiff”, University of Florence,  
18  
19 via della Lastruccia 3, 50019 Sesto Fiorentino, Italy,  
20

21 Phone: +39-055-4573239; Fax: +39-055-4573142; E-mail: [francesco.tadini@unifi.it](mailto:francesco.tadini@unifi.it)  
22  
23  
24  
25  
26  
27

### 28 REFERENCES

- 29  
30  
31 (1) Tadini-Buoninsegni, F.; Bartolommei, G.; Moncelli, M. R.; Fendler, K. Charge transfer in P-type  
32  
33 ATPases investigated on planar membranes. *Arch. Biochem. Biophys.* **2008**, *476*, 75-86.  
34  
35  
36 (2) Schulz, P.; Garcia-Celma, J. J.; Fendler, K. SSM-based electrophysiology. *Methods* **2008**, *46*,  
37  
38 97-103.  
39  
40  
41 (3) Pintschovius, J.; Fendler, K. Charge translocation by the Na<sup>+</sup>/K<sup>+</sup>-ATPase investigated on solid  
42  
43 supported membranes: rapid solution exchange with a new technique. *Biophys. J.* **1999**, *76*, 814-  
44  
45 826.  
46  
47  
48 (4) Lewis, D.; Pilankatta, R.; Inesi, G.; Bartolommei, G.; Moncelli, M. R.; Tadini-Buoninsegni, F.  
49  
50 Distinctive features of catalytic and transport mechanisms in mammalian sarco-endoplasmic  
51  
52  
53  
54  
55  
56  
57  
58  
59  
60

1 reticulum  $\text{Ca}^{2+}$  ATPase (SERCA) and  $\text{Cu}^{+}$  (ATP7A/B) ATPases. *J. Biol. Chem.* **2012**, *287*, 32717-  
2 32727.

3  
4  
5  
6  
7 (5) Bartolommei, G.; Moncelli, M. R.; Rispoli, G.; Kelety, B.; Tadini-Buoninsegni, F. Electrogenic  
8 ion pumps investigated on a solid supported membrane: comparison of current and voltage  
9 measurements. *Langmuir* **2009**, *25*, 10925-10931.

10  
11  
12  
13 (6) Zebrowska, A.; Krysiński, P. Incorporation of  $\text{Na}^{+},\text{K}^{+}$ -ATPase into the thiolipid biomimetic  
14 assemblies via the fusion of proteoliposomes. *Langmuir* **2004**, *20*, 11127-11133.

15  
16  
17  
18 (7) Ganea, C.; Fendler, K. Bacterial transporters: charge translocation and mechanism. *Biochim.*  
19  
20  
21  
22  
23  
24  
25  
26  
27  
28  
29  
30  
31  
32  
33  
34  
35  
36  
37  
38  
39  
40  
41  
42  
43  
44  
45  
46  
47  
48  
49  
50  
51  
52  
53  
54  
55  
56  
57  
58  
59  
60

*Biophys. Acta* **2009**, *1787*, 706-713.

(8) Khafizov, K.; Perez, C.; Koshy, C.; Quick, M.; Fendler, K.; Ziegler, C.; Forrest, L. R.  
Investigation of the sodium-binding sites in the sodium-coupled betaine transporter BetP. *Proc.*  
*Natl. Acad. Sci. U.S.A.* **2012**, *109*, E3035-E3044.

(9) Schulz, P.; Dueck, B.; Mourot, A.; Hatahet, L.; Fendler, K. Measuring ion channels on solid  
supported membranes. *Biophys. J.* **2009**, *97*, 388-396.

(10) Balannik, V.; Obrdlik, P.; Inayat, S.; Steensen, C.; Wang, J.; Rausch, J. M.; DeGrado, W. F.;  
Kelety, B.; Pinto, L. H. Solid-supported membrane technology for the investigation of the influenza  
A virus M2 channel activity. *Pflugers Arch.* **2010**, *459*, 593-605.

(11) Blesneac, I.; Ravaud, S.; Machillot, P.; Zoonens, M.; Masscheylen, S.; Miroux, B.; Vivaudou,  
M.; Pebay-Peyroula, E. Assaying the proton transport and regulation of UCP1 using solid supported  
membranes. *Eur. Biophys. J.* **2012**, *41*, 675-679.

(12) Garcia-Celma, J.; Szydelko, A.; Dutzler, R. Functional characterization of a ClC transporter by  
solid-supported membrane electrophysiology. *J. Gen. Physiol.* **2013**, *141*, 479-491.

- 1  
2  
3  
4  
5  
6  
7  
8  
9  
10  
11  
12  
13  
14  
15  
16  
17  
18  
19  
20  
21  
22  
23  
24  
25  
26  
27  
28  
29  
30  
31  
32  
33  
34  
35  
36  
37  
38  
39  
40  
41  
42  
43  
44  
45  
46  
47  
48  
49  
50  
51  
52  
53  
54  
55  
56  
57  
58  
59  
60
- (13) Ekeröth, J.; Konradsson, P.; Björefors, F.; Lundström, I.; Liedberg, B. Monitoring the interfacial capacitance at self-assembled phosphate monolayers on gold electrodes upon interaction with calcium and magnesium. *Anal. Chem.* **2002**, *74*, 1979-1985.
- (14) Rossetti, F. F.; Bally, M.; Michel, R.; Textor, M.; Reviakine, I. Interactions between titanium dioxide and phosphatidyl serine-containing liposomes: formation and patterning of supported phospholipid bilayers on the surface of a medically relevant material. *Langmuir* **2005**, *21*, 6443-6450.
- (15) Sinn, C. G.; Antonietti, M.; Dimora, R. Binding of calcium to phosphatidylcholine–phosphatidylserine membranes. *Colloids Surf. A* **2006**, *282-283*, 410-419.
- (16) Garcia-Celma, J. J.; Hatahet, L.; Kunz, W.; Fendler, K. Specific anion and cation binding to lipid membranes investigated on a solid supported membrane. *Langmuir* **2007**, *23*, 10074- 10080.
- (17) Monson, C. F.; Cong, X.; Robison, A. D.; Pace, H. P.; Liu, C.; Poyton, M. F.; Cremer, P. S. Phosphatidylserine reversibly binds  $\text{Cu}^{2+}$  with extremely high affinity. *J. Am. Chem. Soc.* **2012**, *134*, 7773-7779.
- (18) Ekeröth, J.; Konradsson, P.; Höök, F. Bivalent-ion-mediated vesicle adsorption and controlled supported phospholipid bilayer formation on molecular phosphate and sulfate layers on gold. *Langmuir* **2002**, *18*, 7923-7929.
- (19) Coronado, R. Effect of divalent cations on the assembly of neutral and charged phospholipid bilayers in patch-recording pipettes. *Biophys. J.* **1985**, *47*, 851-857.
- (20) Eletr, S.; Inesi, G. Phospholipid orientation in sarcoplasmic membranes: spin-label ESR and proton MNR studies. *Biochim. Biophys. Acta* **1972**, *282*, 174-179.

- 1  
2 (21) Lowry, O. H.; Rosebrough, N. J.; Farr, A. L.; Randall, R. J. Protein measurement with the Folin  
3 phenol reagent. *J. Biol. Chem.* **1951**, *193*, 265-275.  
4  
5  
6  
7 (22) Inesi, G.; Toyoshima, C. In *Handbook of ATPases: Biochemistry, Cell Biology,*  
8 *Pathophysiology*; Futai, M., Wada, Y., Kaplan, J. H., Eds; Wiley-VCH: Weinheim, 2004; p 63.  
9  
10  
11  
12 (23) Liu, Y.; Pilankatta, R.; Lewis, D.; Inesi, G.; Tadini-Buoninsegni, F.; Bartolommei, G.; Moncelli,  
13 M. R. High-yield heterologous expression of wild type and mutant Ca<sup>2+</sup> ATPase: Characterization  
14 of Ca<sup>2+</sup> binding sites by charge transfer. *J. Mol. Biol.* **2009**, *391*, 858-871.  
15  
16  
17  
18  
19  
20 (24) Tadini-Buoninsegni, F.; Bartolommei, G.; Moncelli, M. R.; Tal, D. M.; Lewis, D.; Inesi, G.  
21 Effects of high-affinity inhibitors on partial reactions, charge movements, and conformational states  
22 of the Ca<sup>2+</sup> transport ATPase (sarco-endoplasmic reticulum Ca<sup>2+</sup> ATPase). *Mol. Pharmacol.* **2008**,  
23 *73*, 1134-1140.  
24  
25  
26  
27  
28  
29  
30 (25) Guidotti, C.; Minunni, M.; Moncelli, M. R. Probing DNA hybridization in thiolipid  
31 monolayers by means of impedance spectroscopy. *Electrochem. Commun.* **2007**, *9*, 2380-2386.  
32  
33  
34  
35 (26) Møller, J. V.; Olesen, C.; Winther, A. M.; Nissen, P. The sarcoplasmic Ca<sup>2+</sup>-ATPase: design of a  
36 perfect chemi-osmotic pump. *Q. Rev. Biophys.* **2010**, *43*, 501-566.  
37  
38  
39  
40 (27) Sagara, Y.; Inesi, G. Inhibition of the sarcoplasmic reticulum Ca<sup>2+</sup> transport ATPase by  
41 thapsigargin at subnanomolar concentrations. *J. Biol. Chem.* **1991**, *266*, 13503-13506.  
42  
43  
44  
45  
46 (28) Lytton, J.; Westlin, M.; Hanley, M. R. Thapsigargin inhibits the sarcoplasmic or endoplasmic  
47 reticulum Ca-ATPase family of calcium pumps. *J. Biol. Chem.* **1991**, *266*, 17067-17071.  
48  
49  
50  
51 (29) Steinem, C.; Janshoff, A.; Ulrich, W. P.; Sieber, M.; Galla, H. J. Impedance analysis of  
52 supported lipid bilayer membranes: a scrutiny of different preparation techniques. *Biochim.*  
53 *Biophys. Acta* **1996**, *1279*, 169-180.  
54  
55  
56  
57  
58  
59  
60

- 1  
2  
3  
4  
5  
6  
7  
8  
9  
10  
11  
12  
13  
14  
15  
16  
17  
18  
19  
20  
21  
22  
23  
24  
25  
26  
27  
28  
29  
30  
31  
32  
33  
34  
35  
36  
37  
38  
39  
40  
41  
42  
43  
44  
45  
46  
47  
48  
49  
50  
51  
52  
53  
54  
55  
56  
57  
58  
59  
60
- (30) Diao, P.; Jiang, D.; Cui, X.; Gu, D.; Tong, R.; Zhong, B. Unmodified supported thiol/lipid bilayers: studies of structural disorder and conducting mechanism by cyclic voltammetry and AC impedance. *Bioelectrochem. Bioenerg.* **1999**, *48*, 469-475.
- (31) Plant, A. L. Self-assembled phospholipid/alkanethiol biomimetic bilayers on gold. *Langmuir* **1993**, *9*, 2764-2767.
- (32) Bilewicz, R.; Majda, M. Monomolecular Langmuir-Blodgett films at electrodes. Formation of passivating monolayers and incorporation of electroactive reagents. *Langmuir* **1991**, *7*, 2794-2802.
- (33) Tadini Buoninsegni, F.; Herrero, R.; Moncelli, M. R. Alkanethiol monolayers and alkanethiol/phospholipid bilayers supported by mercury: an electrochemical characterization. *J. Electroanal. Chem.* **1998**, *452*, 33-42.
- (34) Kryszinski, P.; Moncelli, M. R.; Tadini-Buoninsegni, F. A voltammetric study of monolayers and bilayers self-assembled on metal electrodes. *Electrochim. Acta* **2000**, *45*, 1885-1892.
- (35) Laredo, T.; Leitch, J.; Chen, M.; Burgess, I. J.; Dutcher, J. R.; Lipkowski, J. Measurement of the charge number per adsorbed molecule and packing densities of self-assembled long-chain monolayers of thiols. *Langmuir* **2007**, *23*, 6205-6211.
- (36) Knoll, W.; Köper, I.; Naumann, R.; Sinner, E.-K. Tethered bimolecular lipid membranes—A novel model membrane platform. *Electrochim. Acta* **2008**, *53*, 6680-6689.
- (37) Homola, J. Surface plasmon resonance sensors for detection of chemical and biological species. *Chem. Rev.* **2008**, *108*, 462-493.
- (38) Brzozowska, M.; Oberts, B. P.; Blanchard, G. J.; Majewski, J.; Kryszinski, P. Design and characterization of novel tether layer for coupling of a bilayer lipid membrane to the surface of gold. *Langmuir* **2009**, *25*, 9337-9345.

1 (39) Tunell, I.; Lim, C. Factors governing the metal coordination number in isolated group IA and  
2  
3  
4 IIA metal hydrates. *Inorg. Chem.* **2006**, *45*, 4811-4819.

5  
6  
7 (40) Oberts, B. P.; Blanchard, G. J. Formation of air-stable supported lipid monolayers and bilayers.  
8  
9  
10 *Langmuir* **2009**, *25*, 2962–2970.

11  
12 (41) Oberts, B. P.; Blanchard, G. J. Ionic binding of phospholipids to interfaces: Dependence on  
13  
14 metal ion identity. *Langmuir* **2009**, *25*, 13025-13033.

15  
16  
17 (42) Oberts, B. P.; Blanchard, G. J. Headgroup-dependent lipid self-assembly on zirconium  
18  
19 phosphate-terminated interfaces. *Langmuir* **2009**, *25*, 13918-13925.  
20  
21  
22  
23  
24  
25  
26  
27  
28  
29  
30  
31  
32  
33  
34  
35  
36  
37  
38  
39  
40  
41  
42  
43  
44  
45  
46  
47  
48  
49  
50  
51  
52  
53  
54  
55  
56  
57  
58  
59  
60



## TOC Graphic

